

Effect of Fibre Properties on Flocculation and Fractionation of Cellulosic Fibres in Dry State

Jaakko Larkomaa, Jouko Niinimäki, Markus Honkanen, Muhammad Hanif, Pentti Saarenrinne

University of Oulu, Finland; Tampere University of Technology

Correspondence To:

Jaakko Larkomaa, email: jaakko.larkomaa@mail.suomi.net

ABSTRACT

This paper investigates a fractionation method of cellulosic fibres in dry state. Although processing of cellulosic fibres in airstream has been utilised for decades in airlaid processes, no attempts to fractionate fibres in dry state have been reported. Our main goal is to determine how fibre properties and fibre consistency affect fibre flocculation and thus the behaviour of fibres in fractionation. Also evaluations of quality and capacity of fractionation operation are made. Pulp flocculation behaviour is measured with digital imaging and image recognition technique before and after the fractionation device. A double-view, orthogonal imaging approach is applied obtaining statistics of three-dimensional shape, dimensions and coordinates of detected fibre flocs. Fraction and fibre properties are determined with Metso Fractionator and Metso Fiberlab. Results show that fibre behaviour in a given system strongly depends on the pulp properties. Flocculation was found to be strongly dependent on fibre consistency. Evaluation of fractionation operation was done with help of calculations of mass-reject rates and separation efficiencies. Calculations showed that highest separation efficiencies can be achieved with system when mass-reject rate is between 0.30 and 0.40.

INTRODUCTION

Cellulosic fibres are commonly processed in dry state in the field of airlaid products. Recently there have also been considerations of finding possibilities to manufacture printing grade papers without using water as an intermediate [1]. Dry state processing of cellulosic fibres requires defibration of pulp to achieve a flow of separated fibres in airstream. These so called fluff pulps are chemically treated with debonding agents before defibration to soften the fibres and to diminish the number of hydrogen bonds

between fibres. This makes defibration easier and minimizes energy consumption.

Airlaid products generally utilise softwood fibres because of their longer fibre length. Mechanical defibration is carried out for example with a hammer mill. Quality of fibres can be controlled by optimizing the hammer mill parameters such as gap width, sieve basket opening and speed of rotation.

In airlaid processes, fibres are transported pneumatically to the former unit after the defibration step (~fibre dispergator) equipped with a mechanical agitation to break fibre flocs and to achieve a smooth fibre layer on wire [2]. It has been reported that longer fibres promote network strength build-up in formation. Network strength can also be affected by friction changing additives and thermal bonding with help of adhesive bicomponent fibres [3].

Fibre properties have huge effect on the properties of end products in both airlaid and conventional papers. Properties of individual fibre are result of wood species, origin and growth season [4]. While carried in airstream fibres have tendency to form fibre flocs. Earlier, while characteristics of cellulosic fibres in airstream have been determined and different flow regimes of fibres: heterogeneous, flocculated, stratified and homogenous have been identified [5].

Fractionation step is used in every wet pulp and papermaking process. Fractionation operations are also widely used in mineral processing sector with both liquid and gaseous intermediates. Evaluation of performance of fractionation operation must be done from both perspectives: fractionation result itself and capacity of operation. However, there have not been earlier considerations to use fractionation procedure in airlaid processes. Appropriate fibre fractionation has great potential to improve the quality of formed fibre layer and therefore the quality of airlaid

products by removing debris such as fibre flocs and undefibrated flakes. This study is the first attempt to fractionate fibres in dry state.

The simplest way to evaluate state of the fibre containing airflow is visual. Other measurement methods to investigate fibre flocculation include e.g. Pulsed Laser Doppler Anemometry (PUD) [6] and Particle Image Velocimetry (PIV) [7]. In this study, fibre flocculation is investigated with a three-dimensional digital imaging approach with the help of mirrors and halogen back-lights obtaining three-dimensional shape, dimensions and coordinates of each detected fibre floc. Fraction and fibre properties are determined with Metso Fractionator and Metso Fiberlab. This work presents how fibre properties affect fibre flocculation and behaviour of fibres in dry-state fractionation.

MATERIALS AND METHODS

Process System

Process system for dry-state fractionation of cellulosic fibres is described in *Figure 1*. The system consists of a feeding hopper, fibre dispergator to break initially formed fibre flocs and a mechanical sieve (i.e. fractionation device) with an agitator to fractionate fibres. The main part of the piping system (shown as red lines in *Figure 1*) is made of conductive and transparent material. Conductive pipes are grounded to minimise the electrostatic forces between fibres and pipe surfaces since the electrostatic forces promotes fibre attachment on the pipe surfaces increasing the flocculation of fibres and may also cause problems in imaging. Flocculation of fibres is investigated at three imaging points: one before and two after the fractionator.

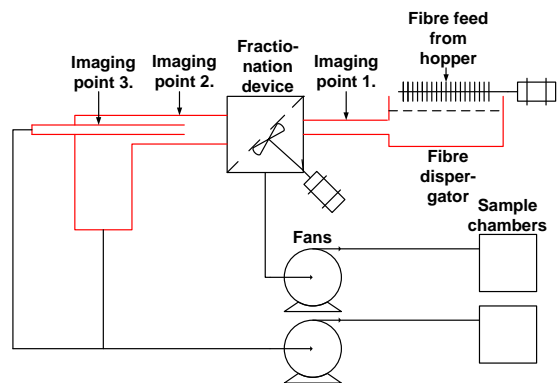


FIGURE 1. Process system for dry-state fractionation of cellulosic fibres.

Fractionation procedure is carried out with an agitated sieve. The sieve is equipped with interchangeable screens with aperture sizes of 0.52, 0.7, 1.7 and 2.0 mm. Screens are 420 mm in diameter, which corresponds to the diameter of the agitator blade diameter. Agitator blades are aligned parallel to the screen 10 mm away from the screen surface. Sieve's agitation speed from 10 to 25 Hz is utilised. Pressure difference over the fractionation device is adjusted to be constant with fans. Finally, samples of accept and reject fraction are collected in sample chambers.

In this work function of fractionation device was evaluated with help of values of mass-reject rate and removal efficiency. Mass-reject rate can be calculated with help of Equation 1 [8].

$$RR_m = \frac{m_R}{m_F} \quad (1)$$

Where RR_m is mass-reject rate
 m_R is mass of reject fraction
 m_F is mass of feed

Removal efficiency can be determined with help of Equation 2.

$$E_R = RR_m \left(\frac{C_R}{C_F} \right) \cdot 100\% \quad (2)$$

Where E_R is the removal efficiency [%]
 RR_m is the mass-reject rate
 C_R and C_F are contents of given components in reject and feed streams

Quality of operation can be easily seen in plotted curves where separation efficiency is represented as a function of mass-reject rate. Single points in fractionation can be evaluated with fractionation index which is presented in Equation 3.

$$Q_k = 1 - \frac{X_I}{X_{II}} \quad 0 < Q_k < 1 \quad (3)$$

Where Q_k is the fractionation index
 X_I and X_{II} refer to quality property in accept and reject fractions

Fibre Material

Pulp for each batch run is fed to fibre dispergator from large fibre hopper via locker feeder for a period of 45 seconds. Pulp is defibrated in advance with Anpap hammer mill having a gap width of 1 mm using one sieve plate with 3 mm apertures and other,

blind sieve plate, with no openings at all. Three different types of pulps are used: eucalyptus (normal type), CTMP (Chemi Thermo Mechanical Pulp, normal type) and softwood (fluff). Pulps are chosen to represent pulps from different manufacturing processes with different fibre properties to clearly see the effects on flocculation and fractionation. *Table 1* shows the properties of the three pulp types after the defibration procedure. Measures are obtained with Metso Fractionator and Metso Fiberlab analysers.

Fibre length and fibre width are most interesting properties in this application because they tell about amount of contact points in between fibres in network within flocs and about fibre flexibility which is another factor affecting network strength [9]. Fibrillation is a value which measures the amount of fibrils on a fibre surface. Fibre curl measures fibre curliness. These values were measured to estimate effects of fibre surface and hooking of fibres to each other.

TABLE I. Initial fibre properties of tested pulp samples

Fibre type	CTMP	Fluff	Euca
Length [mm]	1.64	1.29	0.77
Width [μm]	32.67	21.91	15.75
Curl [%]	10.1	17.0	19.0
Fibrillation [%]	4.96	4.83	6.36

Analysis of Fibre Samples

The fibre samples of accept, reject and feed are collected for further investigation. Samples are weighted and analysed in a laboratory with the help of Metso Fractionator and Metso Fiberlab analysers. Metso Fractionator uses a liquid chromatography method that utilises different residence times of different sizes of fibres and particles in the pipe flow [10]. Larger objects tend to pass through the pipe faster, because they remain in the middle of the laminar pipe flow profile. Fibre containing flow is passed through light beam which is partly depolarised and absorbed due interactions with fibres. Absorption and depolarisation curves are utilised in the estimation of fibre fraction properties. From these two, the depolarisation signal is more sensitive to fibrous material and it is used in this work.

Analysis of Fibre Flocs

Flocculation behaviour of cellulosic fibres is measured with digital imaging. Three monochrome CCD cameras are utilised to measure fibre flocs simultaneously before and after the sieve. Imaging

location 1 in the input channel reveals the initial rate of fibre flocculation after dispersator. Two orthogonal views of flocs are recorded with one camera (Imperx Lynx 2M30 GigE) and a mirror placed at a 45 degrees angle on top of the channel. Views are illuminated with halogen back-lights to recognise the silhouettes of flocs in the image. Flocs appear in the experimental images as dark shadows on the bright background. *Figure 2* shows the camera setup, an example image and *Figure 3* the result image where detected flocs are circled with green outlines. Flow direction here is from right to left.



FIGURE 2. Camera setup at imaging location 1 right after the dispersator.

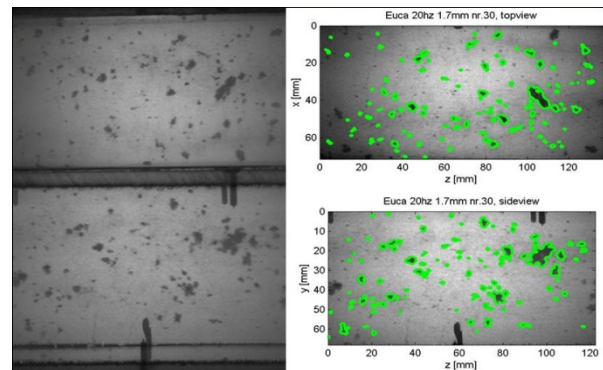


FIGURE 3. Halogen lamps and a mirror provide shadowgraphy-images of top view and side view of flocs in the channel. The original image is shown in the middle and the scaled result image is shown on right.

Camera setup is geometrically calibrated with images of measuring rods to define the correspondence of the target image size in pixels and the target size located inside the flow channel. Pixel scaling depends on the distance between the object and the camera. Here, pixel scaling from 0.096 to 0.108 mm/pixel is

obtained for the side view and 0.108-0.120 mm/pixel for the top view. Therefore, the scaling of objects in the image varies 10% depending on the location of the object in the channel. Objects closer to camera have higher scaling. An initial step is to crop the side view and the top view from the original image and scale them with their mean scaling factors. In addition, the top view (i.e. mirror image) is flipped along its horizontal axis. Then, individual scaling factor is given for each floc that is recognized in both views and whose three-dimensional location in the channel is measured. Finally, three-dimensional floc images are reconstructed and their three-dimensional size, shape and orientation are measured with the help of image recognition algorithms, similar to [11,12].

Floc images are recognised from both projections with a two-step segmentation algorithm that utilises local information on image grey level and grey level standard deviation. It is assumed that floc images appear as dark spots in the image (See *Figure 2*) and that the image grey level varies significantly normal to the edge of the floc image. First, the image is pre-processed providing equalised image where image background has value zero and the darkest floc shadow has value 100. Local (5x5) standard deviation of grey values in the equalised image is segmented with a “focus” threshold value to distinguish the sharp edges of flocs from the image. Then the equalised image is segmented using a constant grey

level threshold of value 40. Grey level segments are then processed one by one as follows:

- Each segment area is re-segmented based on the mean grey level value of the sharp edge regions inside the segment. This procedure effectively responds to the local variation of grey level in the image.
- The second segmentation step sets an individual grey level threshold value for each floc image. It is assumed that grey level on flocs outline is constant and that the grey level standard deviation has its maximum on that location.
- If these assumptions are true, image segmentation has been carried out with grey level threshold value that is individually optimised for every floc, and the floc outlines have been captured with high accuracy.

Detected floc images in both views are paired based on the flocs z-coordinate and z-dimension that are visible in both views. The z-axis is orthogonal to the channel cross-section and parallel to the epipolar lines of the double-view geometry of the imaging system. Two orthogonal projections of each floc provide us a simple way to reconstruct a three-dimensional floc image and to estimate the three-dimensional floc dimensions and coordinates, floc surface area, volume and shape factor. *Figure 4* shows two examples of reconstructed three-dimensional floc images.

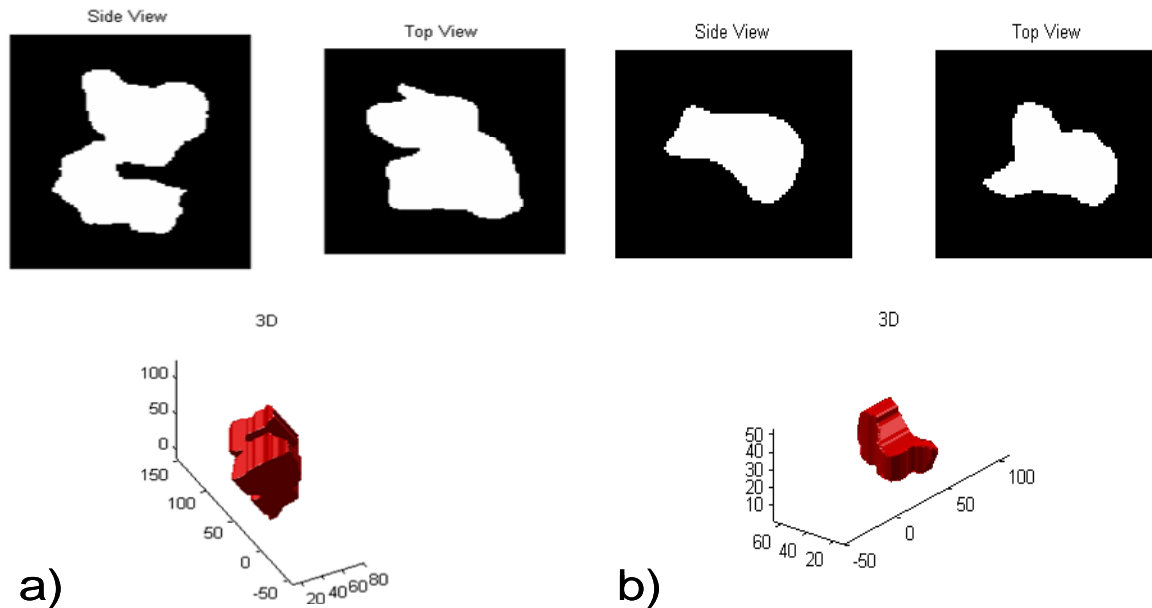


FIGURE 4. Two examples of three-dimensional floc images that are reconstructed from two, orthogonal projections shown on top of the 3D-image.

The presented 3D-imaging technique is also applied at imaging location 2 that is located in the channel right after the fractionator. However, the digital camera (JAI RM4200 GigE) in this location suffered from high noise level and low contrast. The uncertainties related to image analysis restrict the analysis to only one view. The image scaling in the side view varies between 0.112 and 0.129 mm/pixel, which causes 15% measurement uncertainty. The projected area diameter d_a of each detected floc is measured finding a sphere

with diameter d_a , whose cross-sectional area equals to flocs projected area. When irregularly-shaped flocs are randomly distributed and oriented in the channel, the statistics of projected area diameter correspond well to the statistics of the real floc diameter. One-view geometry is also applied in the imaging location 3 further in the channel. There, a high-resolution camera system with AVT Marlin F145b FireWire camera is utilized with 0.0586 mm/pixel scaling and $\pm 5\%$ uncertainty. Even the smallest flocs and fibres with a characteristic dimension larger than 0.1 mm are recognized in the imaging point 3.

RESULTS AND DISCUSSION

Flocculation Behaviour Of Pulps

Flocculation behaviour of fibres depends remarkably on the fibre concentration in flow. Table II lists the measured average fibre concentration, floc concentration, number-average and volume-average floc diameter and maximum floc diameter for each fibre type.

TABLE II. Measured floc concentration and size parameters for each fibre type at imaging point 1. Values are computed as mean in all cases.

Fibre type	CTMP	Fluff	Euca
Fibre concentration [g/m ³]	3.87	3.84	5.81
Floc concentration [pcs/image]	8.62	5.11	28.21
Arithmetic mean [mm]	1.82	2.02	1.84
Volumetric mean [mm]	6.22	6.35	5.92
Maximum [mm]	15.39	15.2	19.88

Visual inspection showed that fibre flocs are mainly formed on the solid surfaces of the process system. Fibres attach to the surface, form flocs and detach

when the aerodynamic drag grows high enough. Air flow is turbulent and has a velocity of about 30 m/s. Flocs are formed inside the dispergator and the fractionator, but some attach themselves on the surfaces of the piping system especially after the fractionator, where the channel cross-section is larger and the flow velocity slower than before the fractionator. Flocculation also takes place at the entrance of the inner accept channel located inside the larger accept channel (see *Figure 1*). The sharp leading edge of the inner channel collects fibres and causes some fibre flocculation. Fibre flocculation can only be prevented by well grounded piping system with constant or decreasing cross-sectional area (flow deceleration should be avoided) and smooth pipe surfaces that do not contain any brackets where fibres might entangle.

Three-dimensional imaging measurements provide plenty of information on the nature of flocs and their movement in air stream. *Figure 6* shows the shape factor curves and floc distributions in the channel cross-section for all fibre types. Floc shape factor is defined as a ratio of floc volume and volume of the bounding box that surrounds the floc. Here, the mean shape factor is plotted as a function of floc diameter. The floc shape becomes more complex with increasing floc size. The same trend is visible for all fibre types. In fact, the shape of the formed flocs is not dependent on the fibre type, but only on floc size and flow conditions in the channel.

Spatial floc distributions show how flocs are distributed in the channel cross-section. Eucalyptus flocs are well distributed over the whole channel having its maximum at the centre of channel cross-section. In the case of fluff and CTMP pulps, flocs are flowing more often on the front and bottom side of the channel. Actually, all fibre types show an increased probability for floc detection at a channel height 50 mm (corresponding to 15 mm below the centre line). This can also be seen in experimental images as streams of flocs and fibres moving in a vortex-type flow structure. The fixed vortex is caused by the dispergator, whose rotating direction defines the location of the vortex in the channel cross-section. Therefore, the distributions in *Figure 6* reveal that CTMP flocs follow the air flow more persistently than fluff and euca flocs.

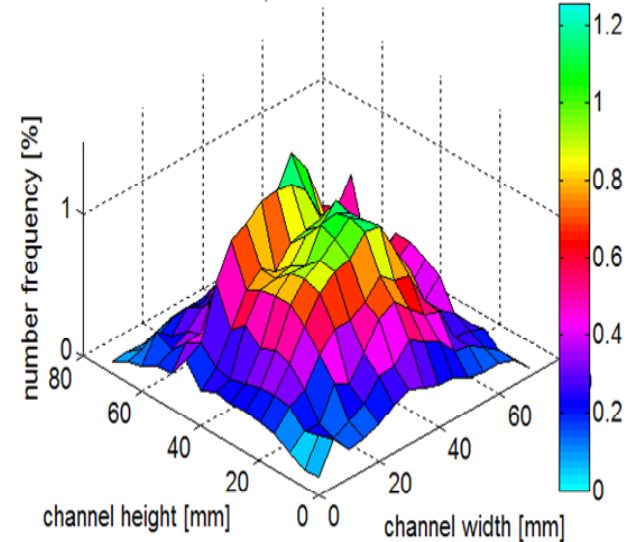
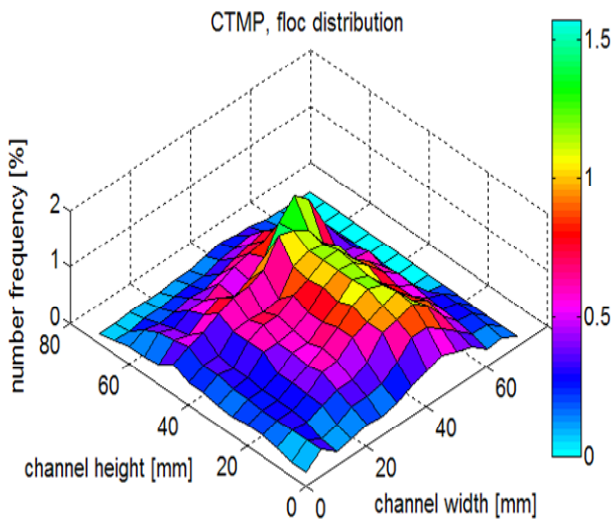
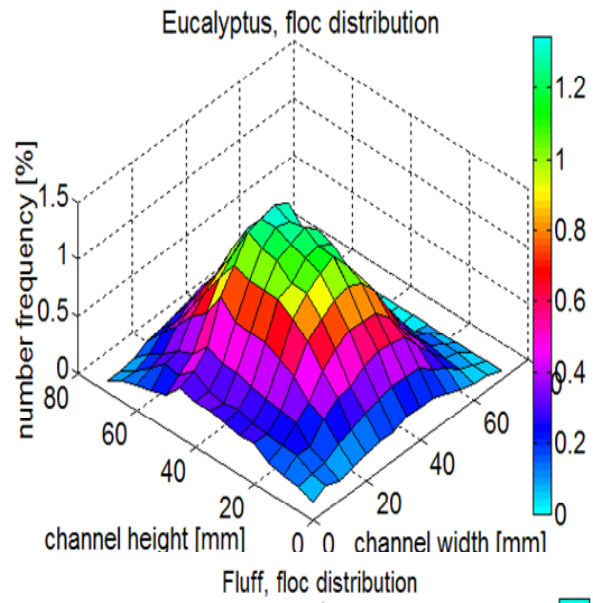
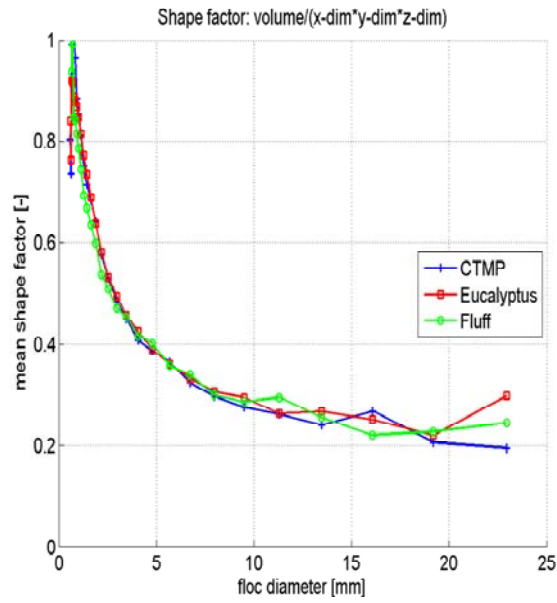


FIGURE 5. Shape factor curve and floc distributions in the channel cross-section for all fibre types at imaging location 1. The number frequency distributions are computed over all measurement cases.

Imaging location 3 in the last channel was photographed with high resolution to even the smallest flocs and fibres with a characteristic dimension of 0.1 mm. *Figure 6* shows the arithmetic and volumetric size distributions of flocs in each measurement case. With CTMP fibres it can be seen that larger holes in sieve

allow larger flocs pass. Otherwis it is difficult to determine effects of parameters because of wide deviations in results. While comparing behaviour of different pulps eucalyptus fibres show smaller floc sizes at this stage of the process. This result is logical while considering fibre lengths of tested pulps.

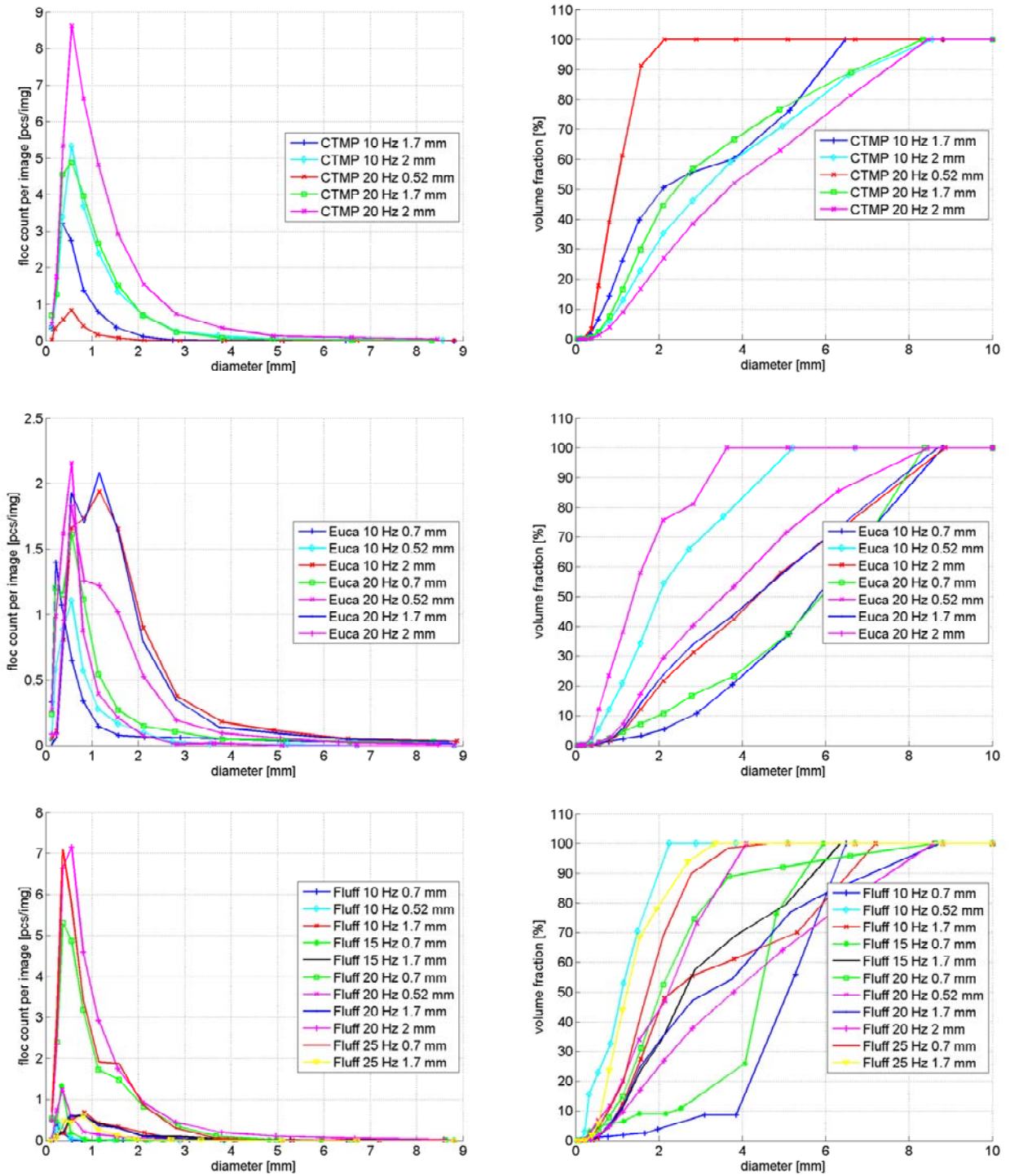


FIGURE 6. Floc size distributions in imaging location 3. The absolute floc count per image is shown on left and the cumulative floc volume distribution on right.

Analysis Of Fibre Properties Of Fractions

Outcome of a dry-state fractionator device depends on the input material properties. Earlier work in this field has showed that pulp manufacturing process and especially fibre aspect ratio have a great effect on the strength of fibre networks in dry cellulosic fibre flocs [13]. Fibre fractions were analysed according to fibre length, width, curl and fibrillation. Altogether 16 tests were made to each pulp with different combinations of

agitation speed, pressure difference and sieve hole size. Test parameter combinations are presented in Table III.

With each pulp it can be seen that there are differences in fibre properties of fractions. Clearest difference can be seen with the longest and stiffest CTMP fibres. With fibre curl it can be seen that accept fraction presents lower values with each pulp. Fibrillation is slightly higher in accept fraction also with all pulp types.

TABLE III. Combination of test parameters used in fractionation

Run no.	Frequency [Hz]	Hole size [mm]	Pressure difference [Pa]
1.	5	0,52	80
2.	30	0,52	80
3.	30	0,52	150
4.	5	0,52	150
5.	5	0,71	80
6.	30	0,71	80
7.	30	0,71	150
8.	5	0,71	150
9.	5	1,7	80
10.	30	1,7	80
11.	30	1,7	150
12.	5	1,7	150
13.	5	2	80
14.	30	2	80
15.	30	2	150
16.	5	2	150

Despite use of different pressure differences and agitation frequencies at first stage results were estimated only as an average of all 16 fractions. Fibre properties of fractions are presented in Table IV.

TABLE IV. Fibre properties of each fraction

Fibre type	Fraction	length [mm]	width [μ m]	curl [%]	fibrillation [%]
CTMP	feed	1,64	32,67	10,08	4,96
	accept	1,35	30,90	9,87	5,12
	reject	1,83	33,44	10,57	4,69
Fluff	feed	1,29	21,91	17,00	4,83
	accept	1,17	21,11	16,00	5,07
	reject	1,27	21,61	16,56	4,95
Euca	feed	0,77	15,75	19,00	6,36
	accept	0,77	15,68	18,19	6,15
	reject	0,79	16,01	18,92	6,12

Fractionation Performance Evaluation

Quality of fractionation is evaluated with the determined depolarisation curves of each fibre fraction. Depolarization signals of CTMP, euca and fluff pulps are presented in Figures 7-9, respectively.

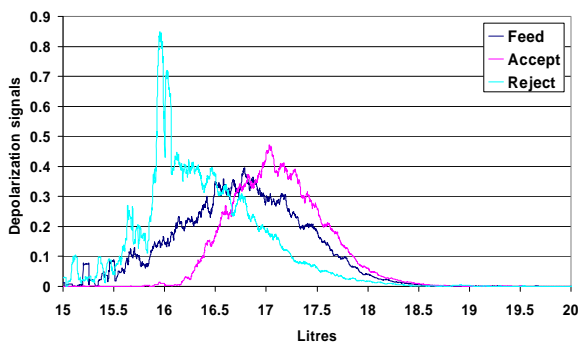


FIGURE 7. Depolarization signals of each fraction with CTMP pulp (5 Hz, 0.71 mm, 80Pa)

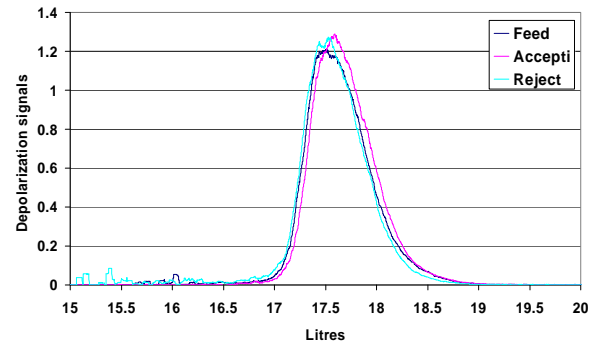


FIGURE 8. Depolarization signals of each fraction with eucalyptus pulp (5Hz, 0.71 mm, 80 Pa)

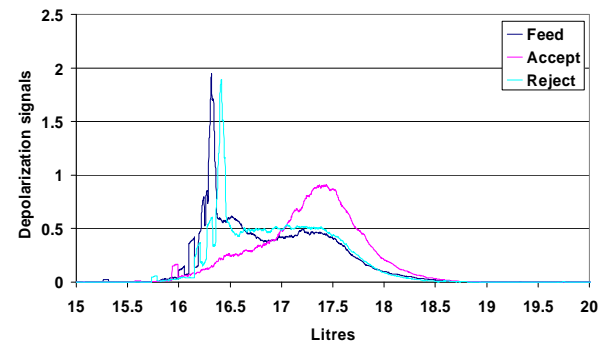


FIGURE 9. Depolarization signals of each fraction with fluff pulp (5 Hz, 0.71 mm, 80 Pa)

From Figures 7-9 it can be seen that dry fractionation works well with both CTMP and fluff pulps, but fails with eucalyptus pulp. However it must be taken into consideration that this type of evaluation is qualitative and does not tell anything about the quantitative system properties i.e. capacity of the fractioning. The same depolarization signals are obtained for feed, accept and reject fractions of eucalyptus fibres. This is probably because of high tendency of eucalyptus fibres to flocculate and also small dimensions of this fibre type. Larger particles, which in case of dry refined cellulose can be undefibrated flakes or fibre flocs, cause spikes on depolarization signal curves. In Figure 10 it can be clearly seen how these large particles are separated to reject fraction.

Fractionation quality is assessed with depolarization curves computing the cumulative surface area of the curve below 16.25 litres. This value 16.25 L is chosen to represent area where the presence of fibre flocs and undefibrated fibre flakes ends and it is used in capacity evaluations as a value for C_R and C_F . Initial content values for all three fractions are presented in Table V.

TABLE V. Initial content of pulp fractions determined from depolarization curves of Metso fractionator

Fibre type	C_F	C_A	C_R
CTMP	43.8	36.9	52.5
Fluff	30.1	33.3	34.0
Euca	36.9	35.1	43.3

While evaluating the performance of fractionation operation separation efficiencies were determined and curves were performed as a function of mass-reject rate, shown in *Figures 10-12*.

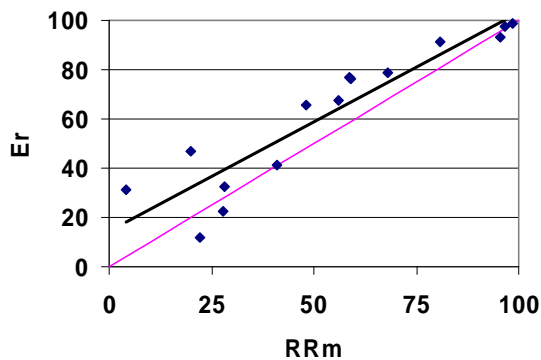


FIGURE 10. Separation efficiency as a function of mass-reject rate with eucalyptus fibres

With eucalyptus fibres it can be seen that there is clear difference between calculated points and a pink line which describes situation where actual separation starts. Linear evaluation shows that best values for separation can be achieved with low reject rates. Average fractionation index for this separation was 0.3.

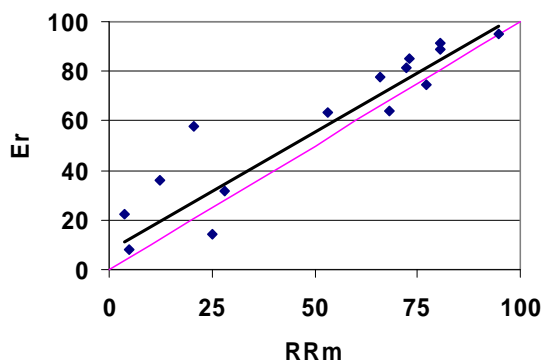


FIGURE 11. Separation efficiency as a function of mass-reject rate with CTMP fibres

CTMP fibres fractionate similarly with eucalyptus fibres. With CTMP average fractionation index is 0.3. Also in this case it was seen that low reject rates enhance separation.

With fluff fibres there were no great differences between accept and reject fractions. Calculated fractionation index showed value -0.1 which means that not actual separation occurs in this operation. It can be withdrawn here that used fractionation operation does not work with debris that fluff pulp contains. Larger particles that are carried with fibres are not undefibrated flakes but later formed fibre flocs which have smaller dimensions and which are more difficult to separate.

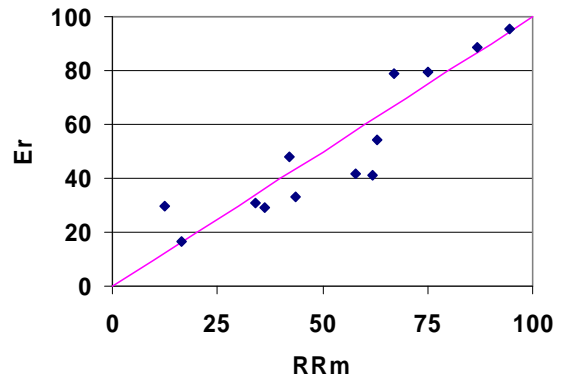


FIGURE 12. Separation efficiency as a function of mass-reject rate with fluff fibres

CONCLUSIONS

Dry-state fractionation of cellulosic fibres produces fibre fractions with specified properties. With all tested pulps and measured fibre properties clear differences between fractions were obtained for all measured properties: fibre length, width, curl and fibrillation. Clearest differences between fractions were achieved with CTMP fibres, in which fibre dimensions are the largest. While evaluating performance of fractionation operation it was seen that best separation efficiencies were obtained with eucalyptus and CTMP fibres. With fluff type of fibres separation did not take place because of low content of undefibrated material in feed fraction.

Flocculation behaviour of the three fibre types (eucalyptus, CTMP and softwood fluff) has been investigated with a three-dimensional digital imaging technique. Results show that fibre flocs are mainly formed on the solid surfaces of the process system. Fibre flocculation can be reduced remarkably by well grounded piping system that has a) a constant or decreasing cross-sectional area to avoid flow deceleration and b) smooth pipe surfaces without any brackets where fibres might attach to. As a summary, the formed flocs of all fibre types have very similar size distributions, but the concentration of flocs varies greatly with the fibre concentration in feed stream. The floc shape becomes more complex as floc size increases. The shape of the formed flocs is not dependent on the fibre type, but on floc size and flow conditions in the channel. The floc imaging results also reveal that the flocs of large CTMP fibres follow the air flow more persistently than the flocs of curly fluff and eucalyptus fibres.

ACKNOWLEDGEMENTS

Authors would like to acknowledge Tekes and Academy of Finland for financing this work.

REFERENCES

- [1] Kononov A., Paulapuro, H. Air Dynamic Forming as an Alternative for Conventional Papermaking, *Paperi ja puu – Paper and timber*, 2004, Vol. 86, No. 4, pp. 243-249.
- [2] Mosgaard J. Dry-Forming: Dan-Web Traces Equipment Evolution, Updates Processes, *Nonwovens World*, Vol. 26, April 1989, pp. 26-27.
- [3] Askling, C., Wågberg, L., Rigdahl, M. Effects of the Process Conditions During Dry-Defibration on the Properties of Cellulosic Networks, *Journal of Materials Science*, 2005, Vol. 33, pp. 2005-2012.
- [4] Sens, D. Fluff Pulp Fibre Morphology Factors for Airlaid Products, *Nonwovens World*, June-July 2003, pp. 45-52.
- [5] Garner G., Kerekes, R.J., Flow Regimes of Wood Pulp Fibres in Air Suspensions, *Tappi Journal*, 1980, Vol. 63, No. 6, pp. 103-107.
- [6] Ek, R., Moller, K., Norman, B. Measurement of Velocity and Concentration Variations in Dilute Fiber/Air Suspensions Using Laser Doppler Anemometer, *Tappi Journal*, 1978, Vol. 61, No. 9, pp. 49-52.
- [7] Melander O., Rasmuson A. Of Lift Forces On Fibre Dispersion, 2007, *International Journal of Multiphase Flow*, Vol. 33, pp. 333-346.
- [8] Körkkö, M., Laitinen, O., Vahlroos, S., Ämmälä, A., Niinimäki, J. Components Removal in Deinking, 8 th Research Forum on Recycling, Niagara Falls, Ontario, Canada.
- [9] Horvath, A.E., Lindström, T. The Influence of Mechanical Surface Linking and Elastic Fiber Bending on Fiber Network Strength, *Nordic Pulp and Paper Research Journal*, Vol. 22, No. 3, 2007, pp. 371-375.
- [10] Laitinen O., Löytynoja L., Niinimäki, J. Tube Flow Fractionator – A Simple Method for Laboratory Fractionation, *Paperi ja Puu – Paper and Timber*, Vol. 88, No. 6, 2006, pp. 1-5.
- [11] Honkanen, M. Direct optical measurement of fluid dynamics and dispersed phase morphology in multiphase flows. Univ. print, Tampere, 2006, pp. 80
- [12] Honkanen, M. & Marjanen, K. Analysis of the overlapping images of irregularly-shaped particles, bubbles and droplets. *Proc. of Int. Conf. on Multiphase Flow*, Leibzig, Germany, paper 559, 2007
- [13] Garner, R.G. Tensile Strength of Dry Wood Pulp Floccs, *Tappi Journal*, 1986, Vol. 69, No. 2, pp. 96-99.

AUTHORS ADDRESSES

Jaakko Larkomaa, M.Sc.; Jouko Niinimäki, Ph.D.
University of Oulu
Department of Process and Environmental Engineering
P.O. Box 4300
University of Oulu, FI-90014
FINLAND

Markus Honkanen, Ph.D.; Muhammad Hanif, M.Sc.; Pentti Saarenrinne, Ph.D.
Tampere University of Technology
FINLAND